Oct 20th, 12:00 AM

Repeated Point Loading Tests on Composite Slabs

Yoshimitsu Itoh

Kiyoshi Komori

Hiroshi Fujioka

Eleventh International Specialty Conference on Cold-Formed Steel Structures
St. Louis, Missouri, U.S.A., October 20-21, 1992

REPEATED POINT LOADING TESTS ON COMPOSITE SLABS

by

Yoshimitsu Itoh *1, Kiyoshi Komori *2, and Hiroshi Fujioka *3

SUMMARY

Single span and double span composite slab specimens were tested by subjecting them to concentrated repeated point loading. From the test results, it was found that the control of concrete cracks caused by the negative moment over the interior support is important in the latter case.

---

*1 Research Engineer, Building Products Development Dept., Nippon Steel Metal Products Co.,Ltd., Tokyo, Japan
*2 Dr. Eng. Professer, Dept. of Structural Engineering, Faculty of Engineering, Univ. of Nagasaki, Japan
*3 Executive Consultant, Nippon Steel Metal Products Co.,Ltd., Tokyo, Japan

REPEATED POINT LOADING TESTS ON COMPOSITE SLABS

by

Yoshimitsu Itoh *1, Kiyoshi Komori *2, and Hiroshi Fujioka *3

ABSTRACT

This paper presents the experimental results of composite slabs subjected to concentrated repeated point loading. Twelve specimens were constructed, including nine specimens for repeated point loading and three for static loading. Two kinds of spanning, single span and double span conditions were adopted. Repeated load levels were determined by taking into account the actual conditions of automobiles and fork lift trucks operating on the floor slabs.

For fatigue tests, two million repeated loadings were applied to each specimen. After the repeated loading, static loading was applied until it reached ultimate strength and caused failure. That ultimate strength was compared with that of the same size specimen subjected to static loading only.

1. INTRODUCTION

Composite slabs which consist of concrete and cold-formed steel decking have been used in the floor slab structures of buildings. Composite slabs have been successfully used for offices, schools, and apartment buildings based on design recommendations for composite slabs [2] which were primarily specified by static load conditions. However, designers and engineers have desired to apply composite slabs to floor slab structures such as warehouses and parking garages because composite slabs have many advantages in strength, construction method, economics, etc. Thus composite slabs have already been applied to structures such as warehouses and parking garages despite the lack of information on their behavioral characteristics and strength. Since repeated loading can occur in such applications, the fatigue behaviour of the composite slabs should be taken into consideration prior to application. It has been found that composite slabs are damaged by repeated loading, especially in structures such as warehouses where fork lift trucks operate.

Recently, a few papers related to the study of composite slabs subjected to repeated loading have appeared [4,5,6] . Obviously the resistance and

---

*1 Research Engineer, Building Products Development Dept., Nippon Steel Metal Products Co.,Ltd., Tokyo, Japan

*2 Dr. Eng. Professor, Dept. of Structural Engineering, Faculty of Engineering, Univ. of Nagasaki, Japan

*3 Executive Consultant, Nippon Steel Metal Products Co.,Ltd., Tokyo, Japan

capacity of a particular composite slab system depends upon the individual composite steel decking as related in the research papers listed [1,4,5,6] for both the static load and the repeated loading tests. Therefore, testing under repeated loading is required since no two composite slab systems are the same, i.e., profiles and interlocking systems are different.

The purpose of this paper is to present the experimental results of a composite slab system subjected to concentrated repeated point loading. This experimental study consisted of the automobile test series and the fork lift test series. In this study, the composite steel decks shown in Figure 1 were employed for the tests. These decks have a complicated corrugation profile, but they do not have any embossments and/or indentations on the sheets. The tests were carried out by Professor Komori at University of Nagasaki over a three year period.

2. TEST PROGRAM

2.1 Test Program

The following test themes were discussed:

1) The number of cycles,
2) The repeated load levels for each application such as for warehouses and parking garages,
3) The choice of appropriate section specifications for composite slabs for each repeated loading level,
4) The span conditions.

Two million cycles were for the fatigue tests considered reasonable based on information in the report [3] that fork lift trucks in warehouses run in cycles of from ninety thousand to one hundred and eighty thousand per year and in reference to previous research [4,5,6] .

Each repeated loading level for the automobile and the fork lift truck wheel loads was appropriately distinct because fork lift trucks are generally heavier than automobiles and the operating behaviour characteristics are different. The level of repeated loading was decided by the following equation.

$$P_{mr} = \alpha \cdot k \cdot W_T \qquad (1)$$

In the above

P_{mr} =maximum repeated load (ton)

α =weighted load factor;
1.2 for automobile wheel load, 1.5 for fork lift truck wheel load.

k =divided load factor,
0.4 for automobile wheel, 0.5 for fork lift truck wheel.

W_T =W_D+W_L (ton), where W_D is the weight of automobile or fork lift truck, and W_L is superimposed load on each of those.

The weighted load factor of 1.2 for the automobile wheel load comes from

"Specifications for Highway Bridges" [7], and the one of 1.5 for the fork lift truck wheel load was determined through discussion by the authors. Using the above equation, P_{mr} was initially determined to be 1.0 ton based on 2.0 tons in "W" for the weight of the automobile, and 6.0 tons based on 8.0 tons in "W" for the weight of the fork lift truck.

For the test series of automobile wheel loading, the two composite slab sections which were ordinarily used in the field were chosen. One section was a slab depth of 130 mm, and the other one had a slab depth of 155 mm. Welded wire fabric was placed over the specimens for this series. Moreover, for comparing a different slab structure, one reinforced concrete slab specimen was adopted. On the other hand, for the test series of fork lift truck wheel loading, the composite slab sections with maximum section properties were adopted. The sections had a slab depth of 175 mm. Reinforcing steel bars instead of welded wire fabric were placed over the specimens.

For spanning conditions, specimens comprised three single span and eight double span composite slab specimens and one double span reinforced concrete slab specimen. According to the design concept of composite slabs, single span composite slab specimens were tested to obtain results for basic fatigue behavioral characteristics and for the strength of the composite slabs under repeated loading. In actual practice in the field, however, composite slabs are usually constructed as continuous spans. Tests of double span specimens reflected conditions similar to actual practice for serviceability. In addition, double span composite slab specimens were tested to research the fatigue behaviour of composite slabs over the interior support where various reinforcements due to bearing negative moment were placed. Testing both single and double span specimens was to obtain comparative results for both specimens.

2.2 Description of Test Specimens

The dimensions of all specimens are listed in Table 1. Twelve specimens were constructed by using one steel deck panel with a width of 610 mm. The reinforced concrete slab specimen was 600 mm wide. The cross-sections of the specimens specified are described in Figure 2. Those nine specimens for the automobile test series were an individual span length of 2700 mm between supports for both single span and double span specimens. For the fork lift truck test series, three double span specimens were used with a 2500 mm long span between supports.

Materials used for test specimens consisted of cold-formed steel decking, welded wire fabric, reinforcing steel bars, and concrete. Three types of composite steel decks were provided: 50 mm deep x 1.2 mm thick ,75 mm deep x 1.2 mm thick, and 75 mm deep x 1.6 mm thick. All steel decks were supplied with a zinc-coated surface finish (180 grams per square meter). Welded wire fabric was 6 mm in diameter (150 mm x 150 mm mesh) which covered all the nine specimens at a depth of 30 mm in the concrete for the automobile test series. Reinforcing steel bars were deformed bars and were 10 mm and 13 mm in diameter. The reinforcements were employed to reinforce the section of composite slabs above the interior support in the four double span composite slab specimens and the

reinforced concrete slab specimen. Normal density concrete with a minimum compressive strength (f_c') of 1.80 kg/mm^2 was supplied by a local ready-mix plant. The results of material tests are listed in Table 2. The tests were tensile coupon tests for all steel materials and compressive cylinder tests for concrete.

When the specimens were assembled, the steel bearing plate (100 mm wide x 600 mm long x 9 mm thick) was welded to the bottom of the steel decks by ϕ-25 mm puddle welding. The bearing width of the steel decks was 50 mm at the ends of each specimen, and was 100 mm at the interior support. The specimens were cast with supports at regular intervals along their entire length which is normal when making specimens for tests. The slab specimens were stripped, covered with nylon sheet, and kept moist for several days, then air cured until tested. Concrete cylinders for material tests were cured next to the specimens in the same way. All specimens were transported to the laboratory by trailers. As a result of the transportation, one or more cracks were observed on the concrete surface above the interior support of several double span specimens before testing.

2.3 Test Equipment and Instrumentation

The load train consisted of a test frame, specimen, and a Shimazu electrohydraulic servo testing apparatus (maximum capacity of 30 tons). Each test set-up for both the single and the double span specimens is shown in Figures 3 and 4, respectively. The plates welded to the steel decks were rigidly clamped onto the reaction beds which were assembled with H-shaped beams to prevent horizontal and vertical movement. A 200 mm x 200 mm steel plate with a thickness of 19 mm was placed on the specimens, and between the steel plate and the contact surface of the concrete there was a plaster pad to provide uniform and smooth loading. A pin system was equipped on the steel plate.

Instrumentation contained displacement transducers (1 / 100 mm) and electrical strain gauges. As shown in Figures 2, 3, and 4, the displacement transducers to record slab deflections were positioned along the individual midspan centrelines and near the support beds. The displacement transducers were also used for recording the horizontal end-slip between the steel deck and the concrete. The expansive widths of cracking over the interior support were also measured by the displacement transducers (pi type). The strain gauges were attached to the steel decks, the reinforcements, and the surfaces of the concrete. The devices worked by monitoring the behaviour of the specimens, and the data for deflections and strains were recorded. Cracking was observed by the naked eye and the cracking formation was recorded.

2.4 Test Procedure

For static test procedure, the loading was accomplished by applying a concentrated point load at the geometrical centre of the individual slab span for both the single and the double span specimens . The loading was gradually applied to reach the maximum strength. On the other hand, the repeated load tests dealt with the goal of two million cycles under concentrated repeated

point loading. The maximum repeated load levels were initially 1.0 ton and 6.0 tons for the automobile and the fork lift truck wheel loads, respectively. The minimum repeated load levels were 0.1 ton in the automobile test series and 0.2 tons in the fork lift truck test series. Cyclic frequency was from 4 Hertz to 8 Hertz. After repeated loading tests, all specimens were loaded to fail completely under the same static load conditions as the static load only. In the repeated loading tests, the data, through various devices, were recorded at 1, $100x10^3$, and $200x10^3$ cycles, and after that at every $200x10^3$ cycles throughout static load conditions. Specimen behaviour was also monitored during cycling through the same devices.

3. TEST RESULTS

The results for all specimens are summarized in Table 3. The comparison of the experimental and the calculated results is summarized in Table 4. It is the primary intention of this paper to present the behavioral characteristics of the composite slabs involved in concentrated repeated point loading through results from the observations of cracking formation, end-slip, failure mode, deflection, strain, rigidity (slope of load-deflection), and ultimate strength.

3.1 Failure Mode in Static Load

The results of cracking formation of the single span specimen DR-SS-1, are described in Figure 8. A lot of flexural cracking occurred initially in the concrete, then the cracking smoothly extended according to the increment of the load. After that, suddenly a diagonal cracking occurred under the loading point, but the diagonal crack did not reach the top surface of the concrete. Simultaneously, the end-slip occurred and the top flanges of the steel deck buckled where the buckling phenomena was checked by the reverse of the strain throughout the strain gauges attached on the top flange portions of the steel deck (see Figure 10). Despite the end-slip occurrence, after that, the load capacity gradually increased, and finally the specimen failed by compressive collapse of the top surface of the concrete under the load point.

On the other hand, the double span specimens, DR-DS-1 for the automobile test series, and DR-DS-2 for the fork lift truck test series, showed that the flexural cracking first occurred over the interior support. The process of the cracking formation and the end-slip occurrence was similar to that of the single span specimen. After that, the composite sections over the interior support were likely to yield, and then one of the composite sections at the midspan finally failed by the compressive crushing of the concrete.

The typical results of the strains attached to the top and bottom of the slabs and of the end-slip are described in Figures 9 and 11, respectively. Thus the failure mode of both the single and the double span specimens seemed to be flexural.

3.2 Failure Mode in Repeated Loading

First, in the automobile test series, observation of single span specimens, DR-SF-1 and DR-SF-2, revealed the appearance of flexural cracking, and then the flexural cracking slightly extended during cycling. The small amount of the end-slip was observed to be 0.13 mm and 0.15 mm in both specimens, DR-SF-1 and DR-SF-2, respectively after 2.0 million cycles.

In contrast, the double span specimens showed different behavioral characteristics from those of the single span specimens in cycling. In the double span specimens, the flexural cracking first appeared over the interior support during the first cycle, and then the flexural cracking was observed in the area of positive moment during cycling. It was noteworthy that the number of cracks over the interior support was related to the quantity of reinforcements. Typical comparison occurred in specimens DR-DF-1 and DR-DF-2 (see Figure 8). The specimen DR-DF-2 with more reinforcement was observed to have more cracks than specimen DR-DF-1. End-slip behavior is described in Figure 14. The irrecoverable (permanent) end-slip appeared in two patterns: the slight and the comparative end-slip. In particular, from observations of the reinforcing steel bars located over the interior support, some reinforcing steel bars which included welded wire fabric were broken by fatigue during cycling (see Figure 13). The number of cycles at that time is indicated in Table 3.

Next, in the fork lift truck test series, it was impossible to carry out a repeated loading test after 1.4 million cycles on account of the extreme increment of the end-slip on the specimen DR-DF-5 which was subjected to the largest repeated load of P_{mr}=6.0 tons. However, the specimen DR-DF-6, subjected to 4.0 ton repeated loading, showed favorable behavioral characteristics in serviceability because the width of the crack over the interior support expanded only 0.3 mm after cycling (see Figure 19).

Eventually, the specimens for both the single and double span conditions were subjected to static load tests after repeated loading in spite of the end-slip occurrence. The process to failure of those specimens was similar to those of the specimens tested on static load only (see Figures 6 and 7). No separation between steel sheet and concrete was observed.

3.3 Deflection Behavior

Figures 12 and 16 describe the development of the deflections at midspan during cycling. The specimens DR-DF-1 and DR-DF-5, subjected to 1.0 ton and 6.0 ton repeated loading respectively, showed a rapid increment of deflections during cycling after the reinforcing steel bars failed by fatigue. Typical load-deflection curves were plotted in Figures 20, 21, and 22 including the permanent deflections after repeated loading. All specimens, especially single span specimens, despite the end-slip occurrence, showed great ductility without any reduction in loading capacity.

3.4 Strain Behavior of Reinforcements

The development of strains observed through the strain gauges attached to the reinforcements is shown in Figures 13 and 17. It is not definite, but the

reinforcements appear to be critical if the strains developed in more than 1000 μ during cycling. Only the composite slab sections over the interior support had lower properties than the other sections against the moment involved, so it is necessary to locate the appropriate reinforcements into the composite sections over the interior support for the serviceability of composite slab structures since composite slabs are generally constructed with continuous span conditions in the actual field.

3.5 Rigidity Reductions

Figure 15 shows rigidity reductions where the plotting is described in a ratio of both the rigidity at the first cycle and any cycles. It had been predicted apparently that the degree of the rigidity reductions depended on the loading levels and the aspect ratio of the reinforcements (p_t). Moreover, it was significant that the rigidity reductions became less in proportion to the number of the cracks depending on "p_t". It was generally the tendency that the rigidity reductions occurred rapidly in the early cycles, and then came to be stable after 200 x 10^3 to 400 x 10^3 cycles. This was shown by the fact that the flexural cracking appeared to stop expansive forming in the concrete during cycling. In comparing the results of the composite slab specimens and the reinforced concrete slab specimen, the rigidity reductions of the latter specimen were found to be larger than those of the composite slab specimens despite the fact that the reinforced concrete slab was designed to have section properties in rigidity and strength approximately equal to those of the composite slabs (such as in specimens DR-DF-1, DR-DF-2, and DR-DF-3) in the positive moment area. It can be considered that the composite slabs had a higher stirrup effect than the reinforced concrete slab.

The comparison of both the initial rigidity of experimental and calculated results for the single span specimens only is shown in Table 4. The initial rigidity of the composite slabs was computed by beam theory based on the moment of inertia of the composite section based on the uncracked section using the modular ratio of 10. In the evaluation of initial rigidity, the experimental results were nearly equal to the calculated ones for static load conditions.

3.6 Ultimate Strength

Table 4 shows the comparison of the experimental and calculated results for ultimate strength. To compute the ultimate strength based on the results of the material tests and the single span conditions, the following expression was used :

$$P_{uc}=4\cdot M_{uy}/L=4\cdot A_s\cdot f_{yt}(d-a/2) \qquad (2)$$

where, $a=A_s\cdot f_{yt}/(0.85f_c'_t\cdot b_d)$

First, in comparing the experimental and calculated results for ultimate strength for single span specimens, the maximum strength was found to be predictable by the ultimate strength computed by the equation (2) in spite of the differences in loading conditions.

Then, comparing the results of both experimental and calculated ultimate strengthes for double span specimens, the former results were 20 percent higher than the calculated results except for the results of specimen DR-DF-1 because the calculated ultimate strength was computed based on single span conditions. Accordingly, it can be considered that the composite slab sections at the interior support developed some internal moment capacity resisting the negative moment, however, detailed discussions of the degree of the moment capacity are out of the scope of this paper.

4. CONCLUSIONS

1) It was found that the ultimate strength of the single span composite slab specimens could be predictably calculated by equation (2) despite the different loading conditions of both the static load and the repeated point loading. It can at least be said that the ultimate strength of the double span composite slab specimens could be estimated on the safe side by equation (2) based on single span conditions.

2) Comparing the effects of the differences in loading conditions, the results of both the composite slab specimens did not show any differences under both the single and the double span conditions in terms of ultimate strength, ductility and failure mode. However, it was found that a small amount of end-slip and rigidity reductions appeared under the repeated loading.

3) The effects of the spanning conditions appeared. When the reinforcements over the interior support were not appropriate for the double span specimens, the fatigue behavior of the reinforcements, and the number, the formation, and the width of cracking was shown to be worse for behavioral characteristics for the floor slab structures. So it is necessary to locate suitable reinforcements in the composite slab sections over the interior support, and repeated point loading tests are necessary for double span specimens.

4) In test specimens for the automobile wheel load, specimen DR-DF-3 with p_t=0.74% showed that the reinforcements over the interior support did not fail by fatigue until 1.8 million cycles under 1.0 ton repeated point loadings.

5) In test specimens for the fork lift truck load, specimen DR-DF-6 showed that the reinforcement over the interior support did not fail, and especially the expansive width of cracking over the interior support reached only 0.3 mm after 2.0 million cycles under 4.0 ton repeated point loadings.

APPENDIX I. -REFERENCES

(1) ASCE Standard, "Specifications for the Design and Construction of Composite Slabs," published by the American Society of Civil Engineers, New York, New York, October, 1984.
(2) Japanese Standard, "Specifications for the Design and Construction of Floor Structures with Steel Decks," published by THE KOZAI CLUB, July, 1987 (in Japanese).
(3) JLA Standard, "Specifications for Highway Brides," published by the Japan Load Association, 1984.
(4) McCuaig, Laurence A. and Schuster, R.M., "Repeated Point Loading on Composite Slabs," Ninth International Specialty Conference on Cold Formed Steel Structures, St.Louis, Missouri, U.S.A., Nov. 1988.
(5) Schuster, R.M. and Suleiman, R.E., "Composite Slabs Subjected to Repeated Point Loading," Eighth International Specialty Conference on Cold Formed Steel Structures, St.Louis, Missouri, U.S.A., Nov.1986.
(6) Temple, M.C. and Abdel-Sayed, G., "Fatigue Experiments on Composite Slab Floors," Fourth International Specialty Conference on Cold Formed Steel Structures, St.Louis, Missouri, U.S.A.,June 1978.
(7) Yoshinobu Iyama, et. al., "A report of Research for Cracks in Storehouse Slabs on Forklift Running," Architectural Institute of Japan, 1987, pp.31-32 (in Japanese).

APPENDIX-II. -NOTATIONS

A_s Cross-sectional area of steel deck, mm^2 of width (b_d)
A_t Cross-sectional area of negative moment reinforcing steel bar over the interior support, mm^2 of width (b_d)
a Depth of equivalent rectangular stress block, $A_s \cdot f_{yt} / (0.85 f'_{ct} \cdot b_d)$, mm
b_d Width of composite test slab, mm
D Nominal out-to-out depth of slab, mm
d Effective slab depth (distance from extreme concrete compression fiber to centroidal axis of the full cross section of the steel deck), mm
d_d Overall depth of steel deck profile, mm
E_c Modulus of elasticity of concrete, kg/mm^2
E_s Modulus of elasticity of steel, kg/mm^2
f'_c Specified compressive strength of concrete, kg/mm^2
f'_{cs} Tensile test cylinder strength of concrete at time of slab testing, kg/mm^2
f'_{ct} Compressive test cylinder strength of concrete at time of slab testing, kg/mm^2
f_{ut} Measured tensile strength of steel, kg/mm^2
f_{yt} Measured yield strength of steel, kg/mm^2
I_u Moment of inertia of composite section based on uncracked section, mm^4
K_c Calculated rigidity based on I_u, kg/mm
K_e Experimental rigidity at one cycle in static load, kg/mm
k Divided load factor for a wheel
L Length of span, mm
M_{uy} Ultimate moment based on yielding of steel, kg·mm

N_c Number of cycles
N_{cf} Number of cycles at reinforcement failed by fatigue
n The modular ratio, E_s / E_c
P_{ce} Experimental cracking load at first observation, kg
P_{DL} Concentrated load converted from dead load of composite slab, kg
P_e Experimental load at any time during test, kg
P_{mr} Maximum repeated load, kg
P_{uc} Ultimate calculated load, kg
P_{ue} Ultimate experimental load in static load, kg
p_t Reinforcement ratio of reinforcing steel bar area to effective concrete area, $A_t / (b_d \cdot d)$, %
t Steel thickness inclusive of coating, mm
W_D Weight of automobile or fork lift truck, kg
W_L Superimposed load of automobile or fork lift truck, kg
W_T Total weight of automobile or fork lift truck, W_D+W_L, kg
α Weighted load factor
Δ_{sr} Irrecoverable end-slip after repeated loading, mm
Δ_{su} Experimental end-slip at Ultimate load, mm
δ_{er} Irrecoverable midspan deflection after repeated loading, mm
δ_{eu} Experimental deflection at Ultimate load, mm

Notes: 1 kg = 9.80665 N, 1 ton= 9.80665 KN

Table 1. Load Characteristics and Dimensions of Specimens

Specimen Identification	Load Characteristics: Loading Condition	Load Characteristics: P_{mr} - N_c (10^3kg) (cycles)	Steel Deck d_d x t (mm)	Slab Depth D (mm)	Reinforcements	Reinforcement Ratio p_t (%)
For Automobile Wheel Series						
< Single Span :L=2,700mm >						
NO.1 DR-SS-1	Static load	- - -	50 x 1.2	130	ϕ 6-150x150	-
NO.2 DR-SF-1	Repeated load	1.0 - 2.0×10^6	50 x 1.2	130	ϕ 6-150x150	-
NO.3 DR-SF-2	Repeated load	1.5 - 1.0×10^6	50 x 1.2	130	ϕ 6-150x150	-
		2.0 - 1.0×10^6				
< Double Span :L=2,700mm >						
NO.4 DR-DS-1	Static load	- - -	50 x 1.2	130	ϕ 6-150x150	0.27
NO.5 DR-DF-1	Repeated load	1.0 - 2.0×10^6	50 x 1.2	130	ϕ 6-150x150	0.27
NO.6 DR-DF-2	Repeated load	1.0 - 2.0×10^6	50 x 1.2	130	ϕ 6-150x150, and 3-D10	0.74
NO.7 DR-DF-3	Repeated load	2.0 - 2.0×10^6	50 x 1.2	130	ϕ 6-150x150	0.27
NO.8 DR-DF-4	Repeated load	1.5 - 2.0×10^6	75 x 1.2	155	ϕ 6-150x150	0.23
NO.9 RC-DF-1	Repeated load	1.0 - 2.0×10^6	75 x 1.2	130	5-D10(@120)	0.69
For Fork Lift Truck Wheel Series						
< Double Span :L=2,500mm >						
NO.10 DR-DS-2	Static load	- - -	75 x 1.6	175	6-D10(@100)	0.78
NO.11 DR-DF-5	Repeated load	6.0 - 1.4×10^5	75 x 1.6	175	6-D10(@100)	0.78
NO.12 DR-DF-6	Repeated load	4.0 - 2.0×10^6	75 x 1.6	175	6-D13(@100)	1.34

Note (1) Nominal dimensions
(2) Repeated loading tests of specimen NO.11 stopped after 1.4 million cycles.
(3) p_t: reinforcement ratio of reinforcing steel bar area to effective area of slab section over the interior support ($A_t/(b_d \cdot d)$).

Table 2. Test Results of Materials unit:kg/mm²

Specimen Identification		Concrete days	$f_c'_t$	$f_c'_s$	E_c (10^3)	Steel Decks f_{yt}	f_{ut}	E_s (10^3)	Welded Wire Fabric f_{yt}	f_{ut}	E_s (10^3)	Reinforcing Bars f_{yt}	f_{ut}	E_s (10^3)
NO.1	DR-SS-1	34	1.98	0.168	2.30	32.05	37.05	19.1	43.91	57.85	19.1	-	-	-
NO.2	DR-SF-1	50	1.99	0.187	2.12	32.05	37.05	19.1	43.91	57.85	19.1	-	-	-
NO.3	DR-SF-2	85	1.89	0.196	1.72	32.05	37.05	19.1	43.91	57.85	19.1	-	-	-
NO.4	DR-DS-1	35	2.60	-	2.64	31.69	44.49	20.5	67.50	68.38	20.3	-	-	-
NO.5	DR-DF-1	36	2.59	0.155	2.56	27.37	42.30	20.4	49.03	57.35	19.4	-	-	-
NO.6	DR-DF-2	38	2.59	0.184	2.32	27.37	42.30	20.4	49.03	57.35	19.4	-	-	-
NO.7	DR-DF-3	28	2.36	-	2.82	31.69	44.49	20.5	67.50	68.38	20.3	36.50	52.57	18.9
NO.8	DR-DF-4	57	2.72	0.200	2.35	30.42	43.64	22.2	49.03	57.35	19.4	-	-	-
NO.9	RC-DF-1	49	2.69	0.218	2.22	-	-	-	-	-	-	36.50	52.57	18.9
NO.10	DR-DS-2	38	2.38	-	2.61	34.82	45.26	19.2	-	-	-	43.10	50.47	22.1
NO.11	DR-DF-5	43	2.63	-	2.54	34.82	45.26	19.2	-	-	-	43.10	50.47	22.1
NO.12	DR-DF-6	57	2.42	-	2.59	34.82	45.26	19.2	-	-	-	43.10	50.47	22.1

Table 3. Test Results

Specimen Identification	Load Characteristics		Characteristics in Cycling					Characteristics in Static Load			
	P_{mr} (10^3kg)	N_c (cycles)	P_{ce} (10^3kg)	K_e (kg/mm)	δ_{er} (mm)	Δ_{sr} (mm)	N_{cr} (10^3c)	P_{ue} (10^3kg)	δ_{eu} (mm)	Δ_{su} (mm)	Mode of Failur
For Automobile Wheel Series											
< Single Span :L=2,700mm >											
NO.1 DR-SS-1	static load only		1.3	517	-	-	-	4.01	125	3.5	Concrete crush
NO.2 DR-SF-1	1.0	-2.0×10^6	1.0	427	5.5	0.13	-	4.00	108	2.5	Concrete crush
NO.3 DR-SF-2	1.5	-1.0×10^6	1.5	468	4.4						
	2.0	-1.0×10^6	(*1)		6.6	0.15	-	4.07	104	11.6	Concrete crush
< Double Span :L=2,700mm >											
NO.4 DR-DS-1	static load only		(*1)	730	-	-	-	5.46	45	6.8	Concrete crush
NO.5 DR-DF-1	1.0	-2.0×10^6	0.5	1,150	12.0	0.81	200	3.52	75	5.1	Concrete crush
NO.6 DR-DF-2	1.0	-2.0×10^6	0.3	880	3.5	0.17	1800	4.77	69	6.4	Concrete crush
NO.7 DR-DF-3	2.0	-2.0×10^6	(*1)	637	2.8	0.23	400	5.25	24	0.3	Concrete crush
NO.8 DR-DF-4	1.5	-2.0×10^6	0.5	2,580	3.8	0.07	800	5.92	60	5.1	Concrete crush
NO.9 RC-DF-1	1.0	-2.0×10^6	0.4	990	4.9	-	-	3.80	62		Concrete crush
For Fork Lift Truck Wheel Series											
< Double Span :L=2,500mm >											
NO.10 DR-DS-2	static load only		2.03	2,430	-	-	-	11.30	40	7.0	Concrete crush
NO.11 DR-DF-5	6.0	-1.4×10^6 (*2)	2.03	1,910	11.2	3.23	300 (*2)	11.19	50	4.9	Concrete crush
NO.12 DR-DF-6	4.0	-2.0×10^6	(*1)	2,660	3.5	0.75	-	12.98	34	3.6	Concrete crush

Note (1) (*1) indicated that cracks were observed before tests.
(2) (*2) indicated that the repeated loading tests were stopped after 1.4 million cycles because of the extreme end-slip.

Table 4. Comparison of Ultimate Experimental and Calculated Strength, and Comparison of Experimental and Calculated Initial Rigidity for Single Span Specimens only

Specimen Identification	P_{ue} (10^3kg)	P_{DL} (10^3kg)	P_{uc} (10^3kg)	$\frac{P_{ue}+P_{DL}}{P_{uc}}$	K_e (kg/mm)	K_c (kg/mm)	$\frac{K_e}{K_c}$
For Automobile Wheel Series							
< Single Span :L=2,700mm >							
NO.1 DR-SS-1	4.01	0.204	4.38	0.96	517	540	0.95
NO.2 DR-SF-1	4.00	0.204	4.38	0.96	427	508	0.84
NO.3 DR-SF-2	4.07	0.204	4.34	0.98	468	434	1.07
< Double Span :L=2,700mm >							
NO.4 DR-DS-1	5.46	0.204	4.33	1.31			
NO.5 DR-DF-1	3.52	0.204	3.79	0.98			
NO.6 DR-DF-2	4.77	0.204	3.79	1.31			
NO.7 DR-DF-3	5.25	0.204	4.27	1.28			
NO.8 DR-DF-4	5.92	0.228	5.13	1.20			
For Fork Lift Truck Wheel Series							
< Double Span :L=2,500mm >							
NO.10 DR-DS-1	11.30	0.248	9.26	1.25			
NO.11 DR-DF-5	11.19	0.248	9.42	1.21			
NO.12 DR-DF-6	12.98	0.248	9.30	1.42			

Note (1) P_{DL}: concentrated load converted dead load of composite slabs.
(2) P_{uc}: ultimate calculated load under single span conditions.

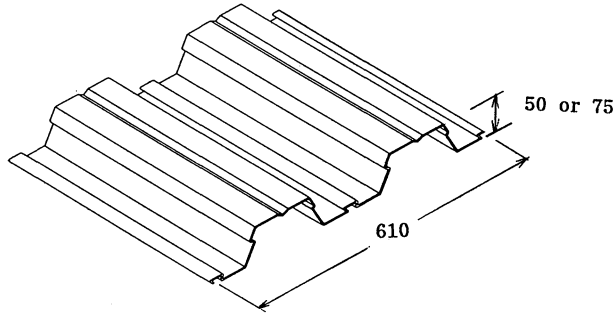

Figure 1. Schematic of Composite Steel Decks Employed

NO.1 DR-SS-1
NO.2 DR-SF-1
NO.3 DR-SF-2
NO.4 DR-DS-1
NO.5 DR-DF-1
NO.7 DR-DF-3

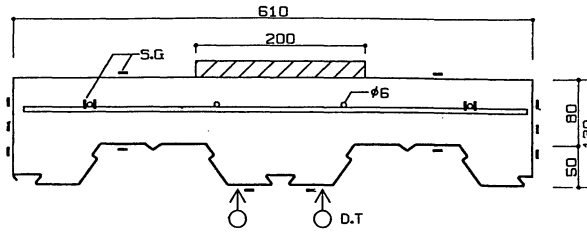

NO.6 DR-DF-2

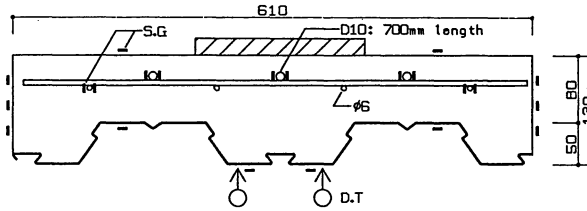

NO.8 DR-DF-4

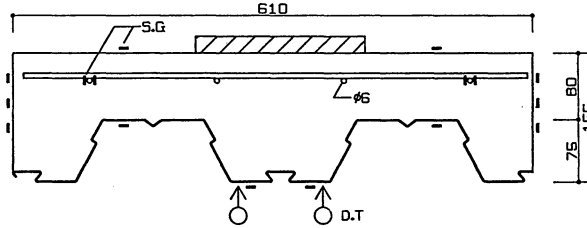

NO.9 RC-DF-1

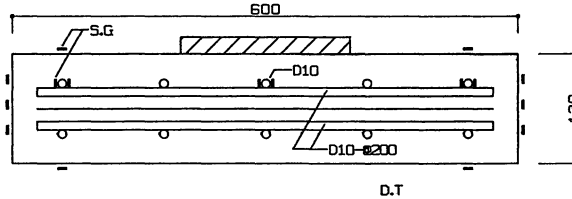

NO.10 DR-DS-2 (D10)
NO.11 DR-DF-5 (D10)
NO.12 DR-DF-6 (D13)

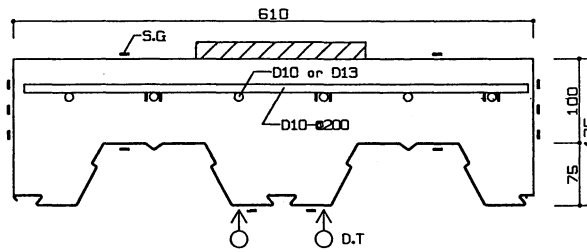

S.G. :Strain Gauge
D.T. :Displacement Transducer

Figure 2. Cross-sections over the Interior Support and Locations of Strain Gauge

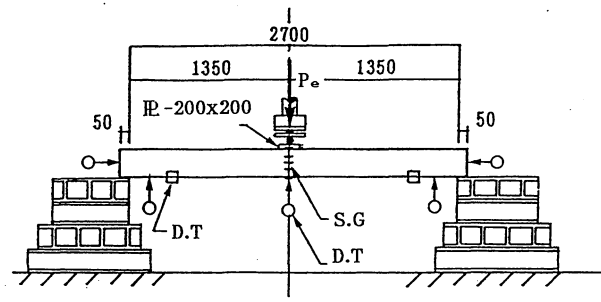

S.G. :Strain Gauge
D.T. :Displacement Tranducer
Dimension :mm

Figure 3. Test Set-up for Single Span Specimens

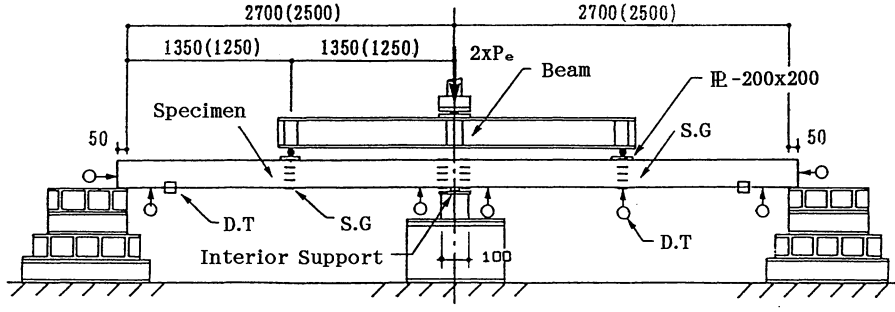

S.G. :Strain Gauge
D.T. :Displacement Tranducer
Dimension :mm

Figure 4. Test Set-up for Double Span Specimens

Figure 5. Photograph Testing the Double Sp Specimen.

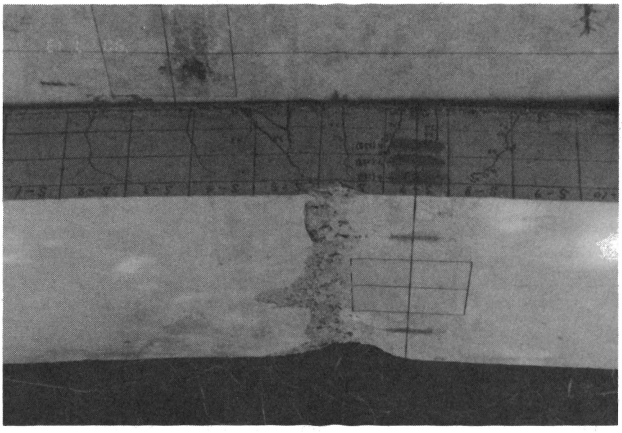

Figure 6. Photograph Cracks over the Inter Support.

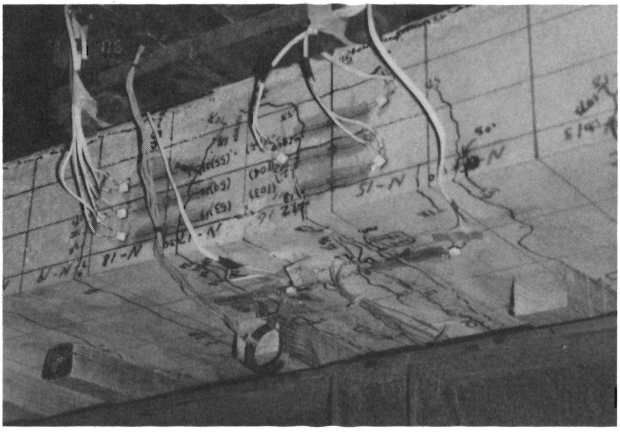

Figure 7.Photograph o Concrete Crush at Mid span

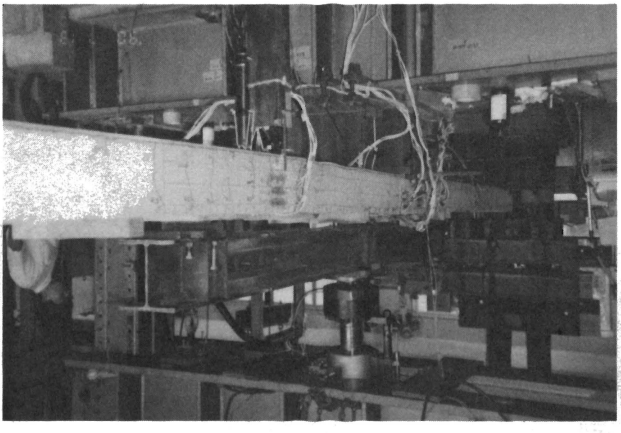

< For Single Span Specimens >

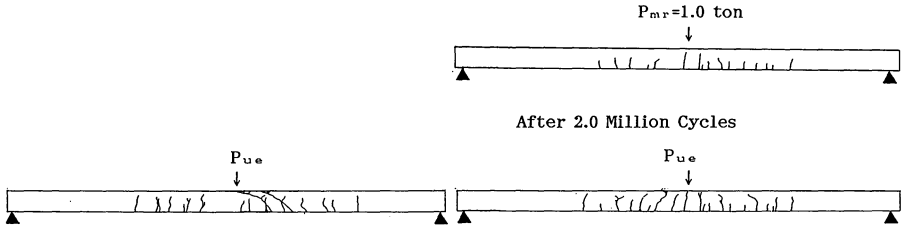

No.1 Specimen DR-SS-1 No.2 Specimen DR-SF-1

< For Double Span Specimens :After 2 Million Cycles >

No.5 Specimen DR-DF-1 (p_t=0.27%)

No.6 Specimen DR-DF-2 (p_t=0.74%)

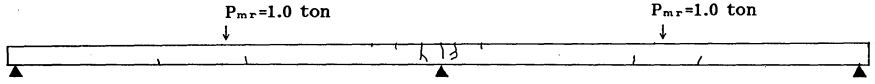

No.9 Specimen RC-DF-1 (p_t=0.69%)

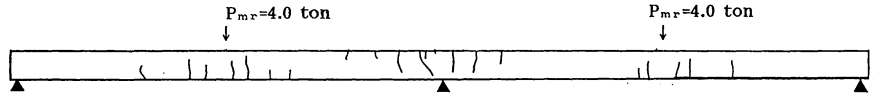

No.12 Specimen DR-DF-6 (p_t=1.34%)

Figure 8. Typical Cracking Formation on the Side of the Concrete

Notes

P_{mr} :Maximum Repeated Load

p_t :Reinforcement Ratio ($A_t/(b_d \cdot d)$) over the Interior Support

P_{ue} :Ultimate Experimental Load

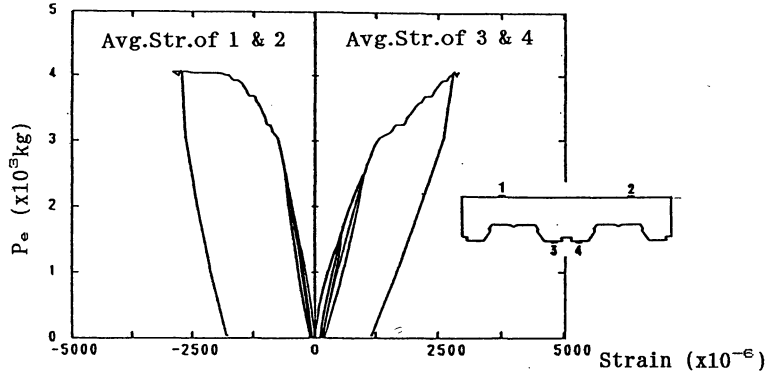

Figure 9. Experimental Strains at the Top & Bottom of Specimen DR-DF-1

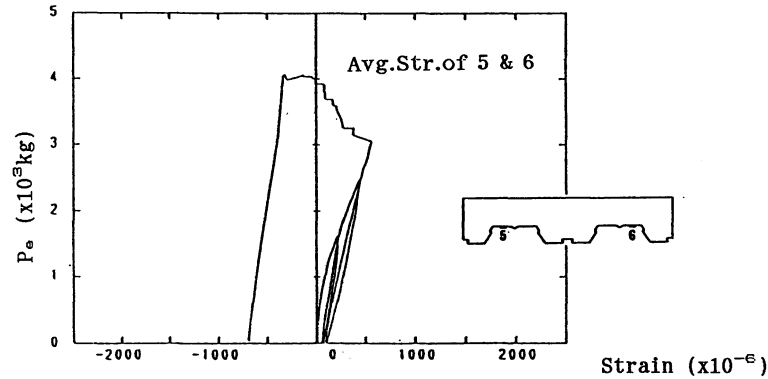

Figure 10. Experimental Strains at the Top Flanges of the Steel Deck of Specimen DR-DF-1

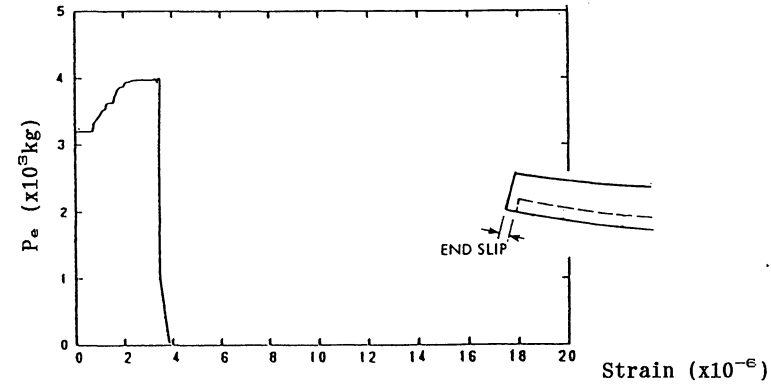

Figure 11. Experimental End-slip of Specimen DR-DF-1

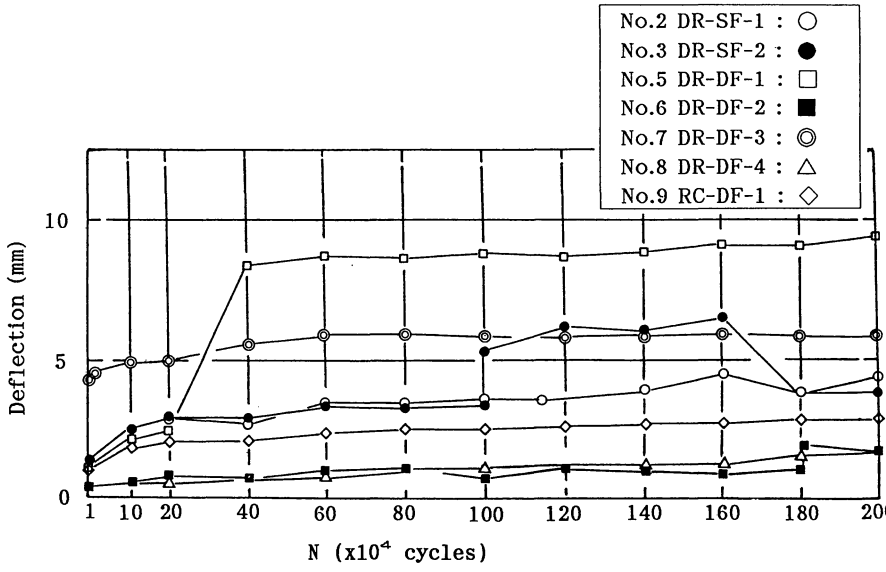

Figure 12. Experimental Deflections at Midspan Versus Number of Cycles of Automobile Test Series

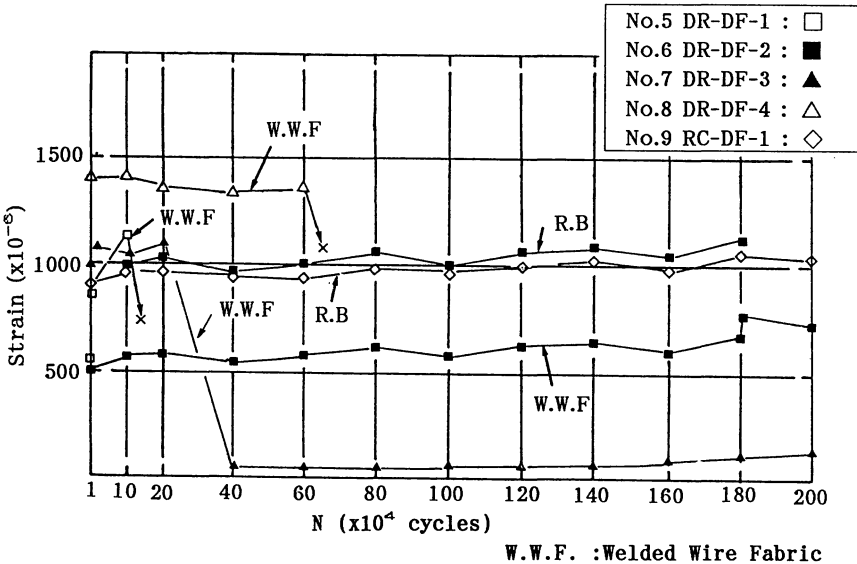

W.W.F. :Welded Wire Fabric
R.B. :Reinforcing Steel Bar

Figure 13. Experimental Strains of Reinforcements over the Interior Support Versus Number of Cycles of Automobile Test Series

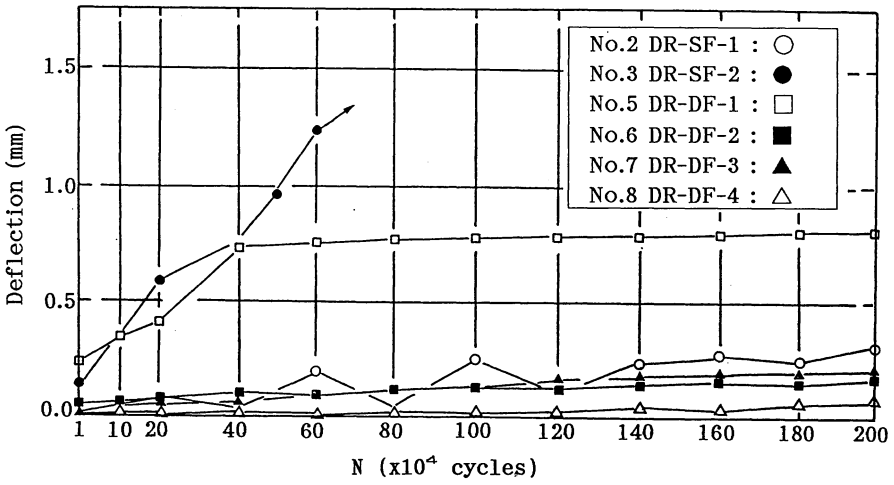

Figure 14. Experimental End-slip Versus Number of Cycles of Automobile Test Series

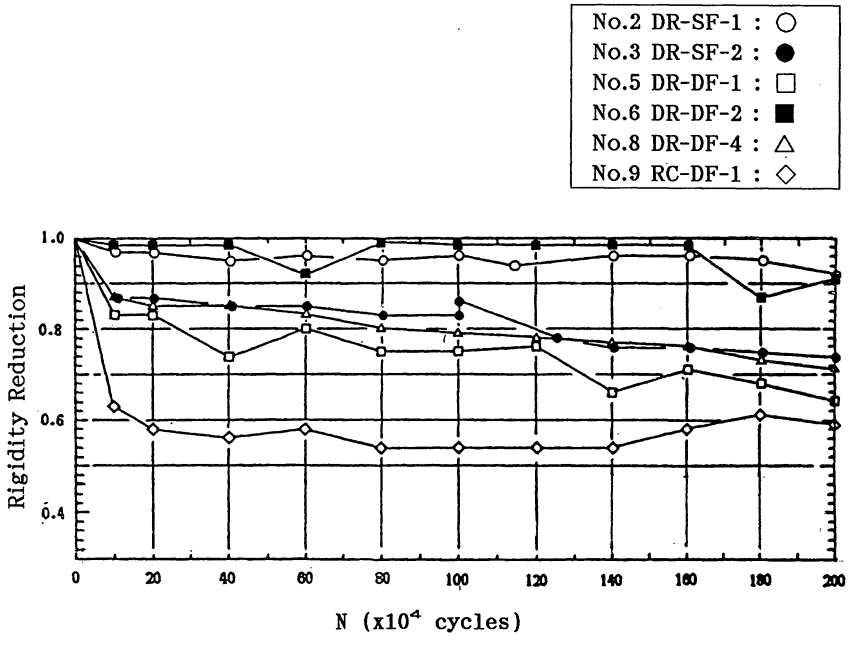

Figure 15. Experimental Rigidity Reductions Versus Number of Cycles of Automobile Test Series

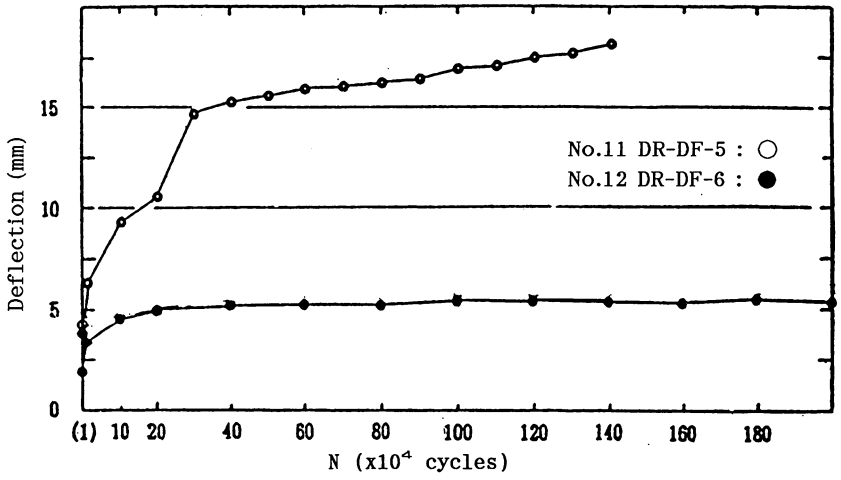

Figure 16. Experimental Deflections at Midspan Versus Number of Cycles of Fork Lift Truck Test Series

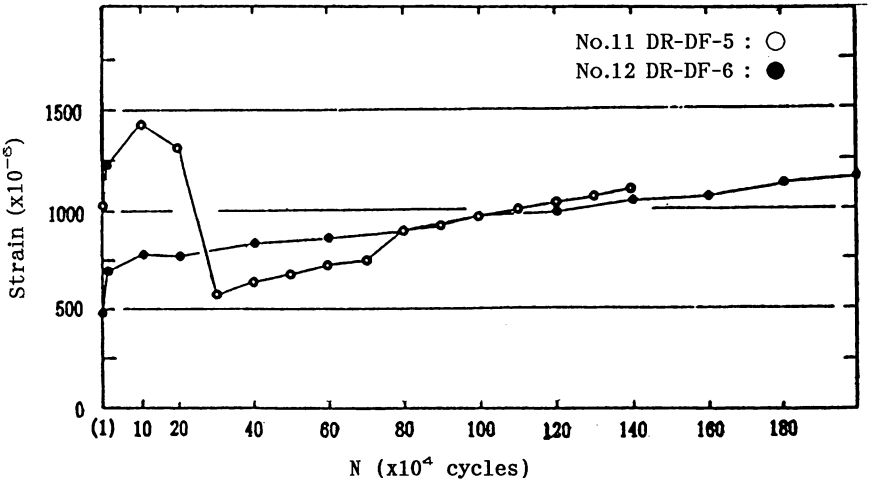

Figure 17. Experimental Strains of Reinforcements over the Interior Support Versus Number of Cycles of Fork Lift Truck Test Series

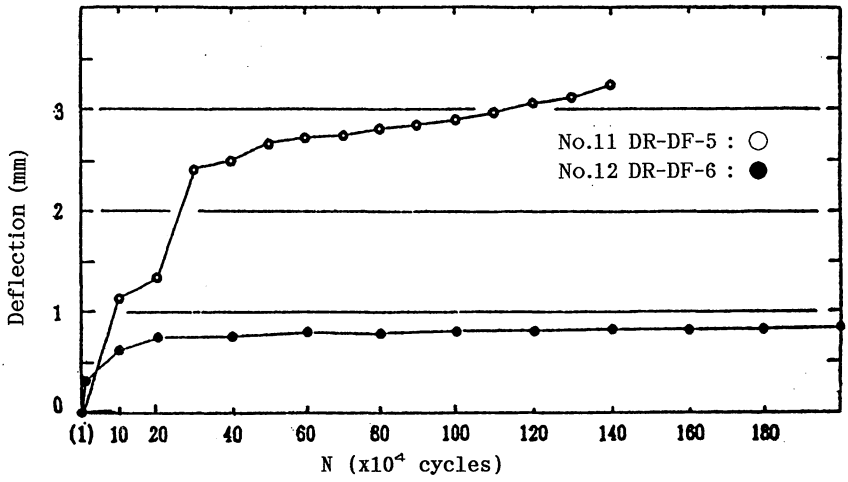

Figure 18. Experimental End-slip Versus Number of Cycles of Fork Lift Truck Test Series

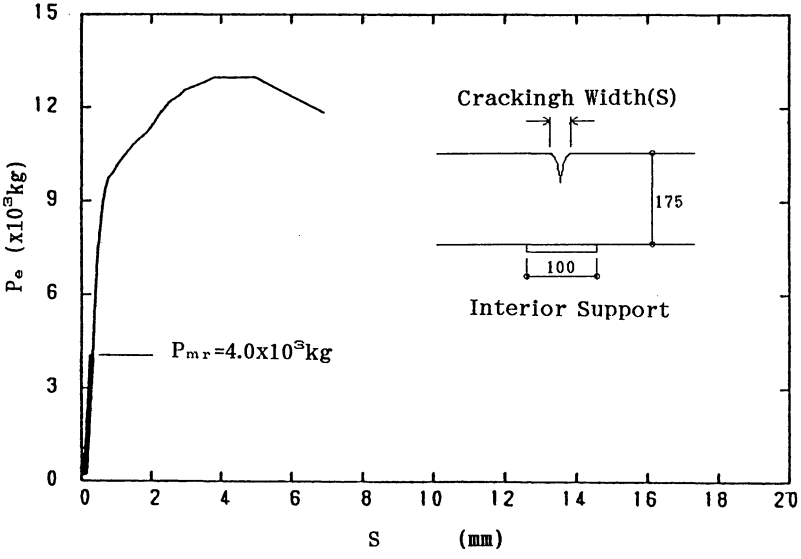

Figure 19. Load Versus Experimental Cracking Widths of Specimen DR-DF-5 of Fork Lift Truck Test Series

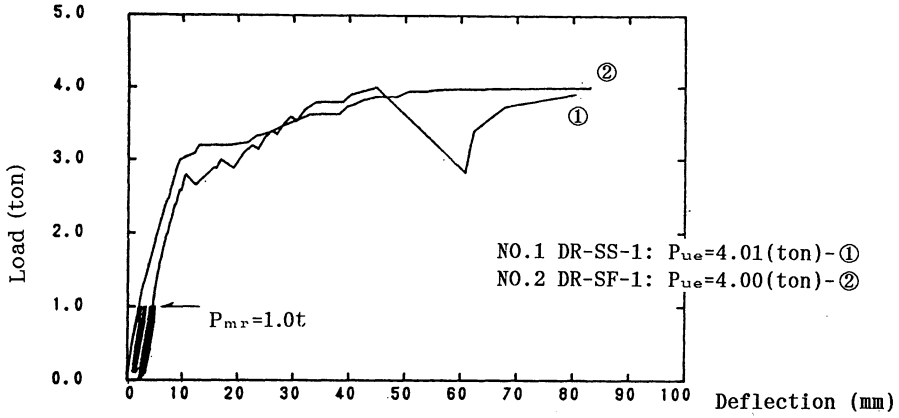

Figure 20. Load-Deflection Curve of Single Span Specimens of Automobile Test Series

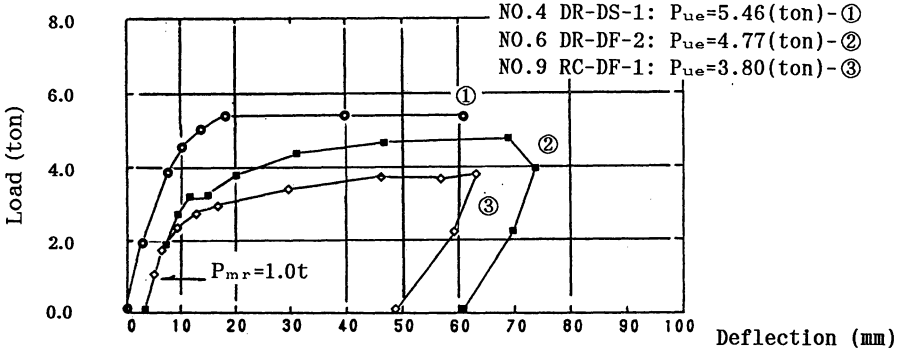

Figure 21. Load-Deflection Curve of Double Span Specimens of Automobile Test Series

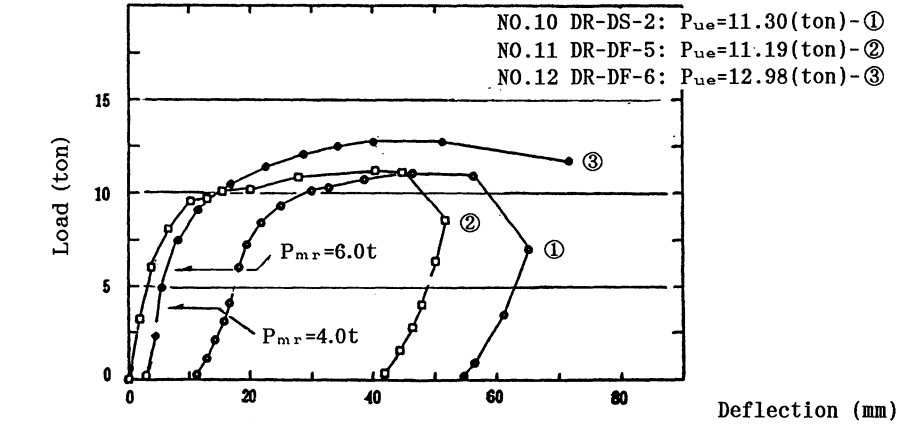

Figure 22. Load-Deflection Curve of Double Span Specimens of Fork Lift Truck Test Series